

Npt2b Deletion Attenuates Hyperphosphatemia Associated with CKD

Susan C. Schiavi, Wen Tang, Christina Bracken, Stephen P. O'Brien, Wenping Song, Joseph Boulanger, Susan Ryan, Lucy Phillips, Shiguang Liu, Cynthia Arbeeny, Steven Ledbetter, and Yves Sabbagh

The Sanofi-Genzyme R&D Center, Genzyme, a Sanofi Company, Framingham, Massachusetts

ABSTRACT

The incidence of cardiovascular events and mortality strongly correlates with serum phosphate in individuals with CKD. The Npt2b transporter contributes to maintaining phosphate homeostasis in the setting of normal renal function, but its role in CKD-associated hyperphosphatemia is not well understood. Here, we used adenine to induce uremia in both Npt2b-deficient and wild-type mice. Compared with wild-type uremic mice, Npt2b-deficient uremic mice had significantly lower levels of serum phosphate and attenuation of FGF23. Treating Npt2b-deficient mice with the phosphate binder sevelamer carbonate further reduced serum phosphate levels. Uremic mice exhibited high turnover renal osteodystrophy; treatment with sevelamer significantly decreased the number of osteoclasts and the rate of mineral apposition in Npt2b-deficient mice, but sevelamer did not affect bone formation and rate of mineral apposition in wild-type mice. Taken together, these data suggest that targeting Npt2b in addition to using dietary phosphorus binders may be a therapeutic approach to modulate serum phosphate in CKD.

J Am Soc Nephrol 23: 1691–1700, 2012. doi: 10.1681/ASN.2011121213

Elevated serum phosphorus even within the normal range is emerging as an important health risk in both normal and CKD populations because it is associated with increased incidence of vascular calcification and mortality.^{1,2} Although current CKD therapies such as phosphate binders effectively decrease serum phosphorus by reducing the pool of absorbable phosphate, management of serum levels remains difficult. A limited understanding of the complexity associated with phosphate regulation has slowed development of optimal therapeutic strategies.

It is well accepted that in normal physiology, the kidney disposes of excess phosphate absorbed by the intestine or released from bone through well characterized, regulated mechanisms. The intestine has been largely viewed as a passive component because the available evidence suggested that the major route of phosphate entry is *via* paracellular transport driven by diffusion.^{3–5} We have recently challenged this dogma by conditionally deleting the intestinal sodium-dependent phosphate cotransporter, Npt2b, in adult mice.⁶ By mimicking

postprandial conditions to maximize contributions of both passive and active transport, Npt2b-dependent phosphate transport was shown to contribute to as much as 50% of the total phosphorus uptake.⁶ Using the everted sac method, we also confirmed that >90% of active transport occurs through Npt2b. Most importantly, Npt2b^{-/-} mice maintained serum phosphorus within the normal range by decreasing the phosphaturic hormone, fibroblast growth factor 23 (FGF23), upregulating renal Npt2a protein expression and subsequently decreasing urinary phosphorus excretion.⁶ These studies demonstrated that Npt2b is an important route

Received December 22, 2011. Accepted June 27, 2012.

Published online ahead of print. Publication date available at www.jasn.org.

Correspondence: Dr. Susan C. Schiavi, The Sanofi-Genzyme R&D Center, 49 New York Avenue, Framingham, MA 01701-9322. Email: susan.schiavi@genzyme.com

Copyright © 2012 by the American Society of Nephrology

for phosphate absorption and participates in the regulation of renal phosphate handling.

Several lines of evidence suggest that inhibition of Npt2b-dependent transport may attenuate the phosphate burden in the absence of a functional kidney. Phosphate lowering effects have been shown in preclinical models and in humans treated with either nicotinamide or its precursor, niacin.^{7–10} Nicotinamide has been shown to inhibit sodium-dependent phosphate transport activity in rat small intestine, reduce Npt2b mRNA expression, and attenuate hyperphosphatemia in an adenine-induced renal failure model.^{11,12} Reduction in serum phosphate with corresponding modulation of Npt2a and 2b mRNA expression has also been observed in rats treated with liver X receptor agonists.¹³ These data cumulatively support the possibility that inhibition of this transporter may be a viable therapeutic alternative. Nonetheless, these agents are also known to have pleiotropic actions, which may also contribute to changes in mineral homeostasis.^{12,14} A recent study in uremic Npt2b^{+/-} mice provides initial evidence that Npt2b reduction specifically decreases hyperphosphatemia.¹⁵ However, because this study was performed using developmental heterozygous mice with ARE, it is unknown whether the effects of Npt2b deletion can be sustained over the course of CKD progression due to upregulation of Npt2a. In addition, bone disease, a known contributor of systemic phosphate burden, was likely not present in this acute model. There are also several inconsistent reports regarding changes in Npt2b expression in uremic models that have generated skepticism for successfully targeting Npt2b in late stage CKD.^{16,17}

In this study, we have examined the long-term effects of reducing Npt2b expression on mineral dysregulation associated with CKD. Hyperphosphatemia was significantly reduced over 5 weeks in uremic Npt2b^{-/-} mice. Furthermore, phosphate binding and Npt2b deletion effects were synergistic as evidenced by serum, urinary, and fecal phosphorus parameters. Significant improvements on bone histomorphometric parameters were also observed in sevelamer-treated uremic Npt2b^{-/-} mice further demonstrating that improved phosphate control led to enhanced benefits on CKD-mineral bone disorder parameters. Taken together, these studies extend previous results by validating the specific role of Npt2b in hyperphosphatemia in a chronic CKD model with high turnover renal osteodystrophy.

RESULTS

Npt2b Expression in Uremic Mice

To assess the contribution of Npt2b to hyperphosphatemia, kidney injury was introduced by adenine treatment of wild-type (WT) or conditional Npt2b^{-/-} mice.⁶ These studies utilized our previously characterized model in which Npt2b deletion in adult mice is driven by a tamoxifen-inducible CRE system.⁶ Parallel studies were performed in animals fed 1% sevelamer carbonate to compare relative effects of deleting

Npt2b with phosphate sequestration. Immunostaining of intestinal sections clearly detected Npt2b protein expression on the villi surfaces of ileum in all WT but not Npt2b^{-/-} mice (Figure 1A). These findings were confirmed by quantitative immunoblot analysis (Figure 1, C and D). A trend toward reduced Npt2b protein expression was observed in uremic WT mice relative to normal mice (Figure 1D). In contrast, sevelamer treatment led to a significant increase in Npt2b protein expression (Figure 1D).

Phenotypic Characterization of Normal and Uremic Mice

Mice with normal kidney function (WT or Npt2b^{-/-}) had similar age-related changes in body weight (Figure 2B), whereas adenine treatment was associated with an approximately 25%–40% reduction in food intake, decreased body weights, and reduced renal function (Figure 2, B and C). Maximal decline in renal function was observed after 2 weeks of adenine treatment with some recovery noted upon adenine withdrawal (Figure 2C). Histologic analysis demonstrated that all uremic groups had moderate to severe renal tubulointerstitial pathology characterized by tubular dilation and/or atrophy, epithelial cell degeneration, necrosis and regeneration, interstitial inflammation, and mild peri-tubular fibrosis (data not shown). There were no detectable differences in renal function across the uremic groups. Histologic analysis of ilial sections from uremic WT or Npt2b^{-/-} mice did not provide evidence of adenine associated toxicity (Figure 1B).

Npt2b Deletion Attenuates Chronic Hyperphosphatemia

WT and Npt2b^{-/-} mice had similar serum phosphate levels as previously described (Figure 3A).⁶ At 2 weeks, WT mice were significantly hyperphosphatemic, whereas Npt2b^{-/-} mice had a slightly lower serum phosphate (Supplemental Figure 1). In contrast, sevelamer treatment led to a significant decrease in Npt2b^{-/-} mice relative to WT treated mice (Supplemental Figure 1). However, after 5 weeks of uremia, WT mice were significantly hyperphosphatemic (6.88 ± 0.31 versus 10.04 ± 0.51 mg/dl), whereas the Npt2b^{-/-} mice had an attenuated increase in serum phosphate levels (10.04 ± 0.51 versus 8.21 ± 0.56 mg/dl). At the dose tested (1%), binder treatment did not alter serum phosphate levels in uremic WT mice (10.04 ± 0.51 , untreated versus 9.67 ± 0.69 , binder-treated mg/dl) but further decreased serum phosphate levels in uremic Npt2b^{-/-} mice (6.88 ± 0.31 ; binder-treated versus 8.21 ± 0.56 mg/dl; untreated) (Figure 3A). Serum calcium levels were similar between WT and Npt2b^{-/-} mice although a statistically significant increase was noted in all sevelamer-treated animals (Figure 3B).

Correlation analysis of serum BUN with serum phosphate of WT and Npt2b^{-/-} mice demonstrated that Npt2b deletion shifts the phosphate slope to the right (Figure 4A). Analysis of the slope of best-fit linear regression for the different treatment groups reveals that uremic WT mice treated with

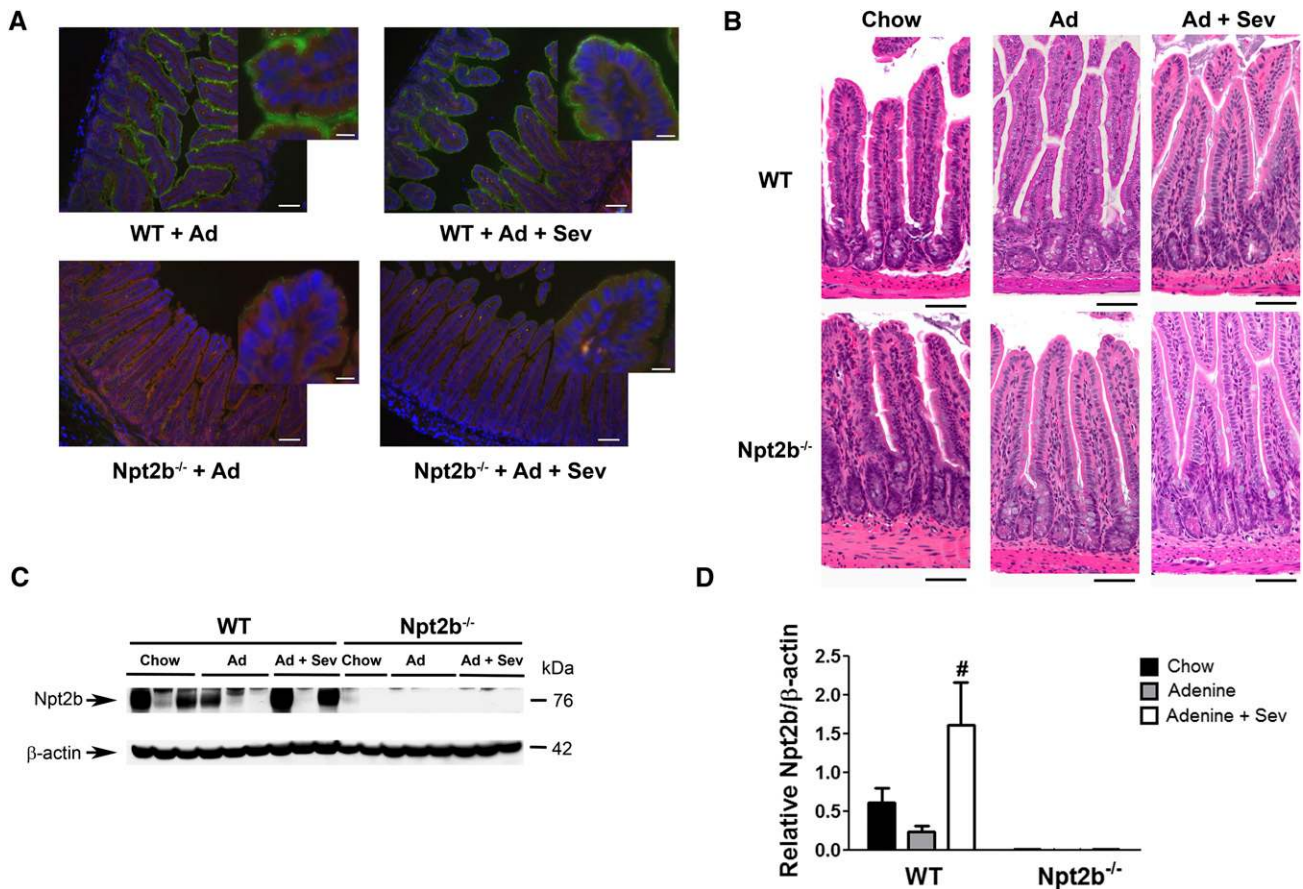


Figure 1. Npt2b expression in mouse ileum. (A) Immunohistochemistry on a cross-sectional area of ileum showing Npt2b protein (green) in uremic WT mice that is absent in Npt2b^{-/-} mice. Hoechst staining for nuclei (blue) and actin staining with phalloidin (red). Expression of Npt2b protein was detected in both untreated and sevelamer (Sev) carbonate-treated WT mice. (B) Hematoxylin and eosin staining of ileum sections from WT and Npt2b^{-/-} knockout mice showing normal villi structure in all the groups. (C) Representative immunoblot for Npt2b protein showing Npt2b expression in WT ileum lysates, which is absent in Npt2b^{-/-} mice. (D) Quantitation of Npt2b protein expression demonstrates significant increase in expression with binder treatment. Data expressed as mean \pm SEM. [#] $P < 0.05$ versus adenine. $n = 8-10$ /group. Scale bar, 50 μm in main image and 10 μm in inset in A; 40 μm in B.

sevelamer carbonate and nontreated uremic Npt2b^{-/-} mice have a decreased slope. In addition, uremic Npt2b^{-/-} mice treated with binder have a significantly lower slope relative to untreated mice (Figure 4B).

The attenuated serum phosphate response in the adenine-treated Npt2b^{-/-} mice was also observed in a second mouse model of CKD, the 5/6 nephrectomy (Nphx) model (Supplemental Figure 2B). The 5/6 Nphx WT mice had a significant increase in serum phosphate correlating with significant changes in BUN, whereas there was no change in serum phosphate in 5/6 Nphx Npt2b^{-/-} mice despite significant changes in renal function (Supplemental Figure 2).

The higher urinary and fecal phosphate excretion due to the higher dietary phosphate content in uremic groups obscured any potential difference between binder-treated and untreated uremic WT mice (Figure 3, C and D). In contrast, binder treatment in uremic Npt2b^{-/-} mice was associated with a significant increase in fecal phosphate excretion (29.39 ± 5.43 versus

45.91 ± 5.91 mg/d) with a corresponding decrease in urinary phosphate excretion (9.12 ± 0.48 versus 6.15 ± 0.60 mg/d) (Figure 3, C and D). These results suggest that binder treatment in combination with Npt2b deletion was associated with more robust phosphate control that translated to statistically significant changes in serum, urine, and fecal phosphate levels.

Parathyroid hormone (PTH) was significantly elevated in all uremic groups relative to nonuremic mice (Figure 5A). A non-statistical trend toward decreased PTH levels was observed only in binder-treated uremic Npt2b^{-/-} mice (Figure 5A). Serum FGF23 levels were significantly elevated in uremic WT and Npt2b^{-/-} mice relative to nonuremic mice although Npt2b^{-/-} mice had a 30% lower level of FGF23 (Figure 5B). Sevelamer carbonate treatment in uremic WT mice led to a 22% decrease in FGF23 levels, although this was not statistically different from untreated WT mice (Figure 5B). In contrast, a 50% significant reduction in FGF23 levels was observed in binder-treated compared with untreated uremic Npt2b^{-/-} mice (Figure 5B).

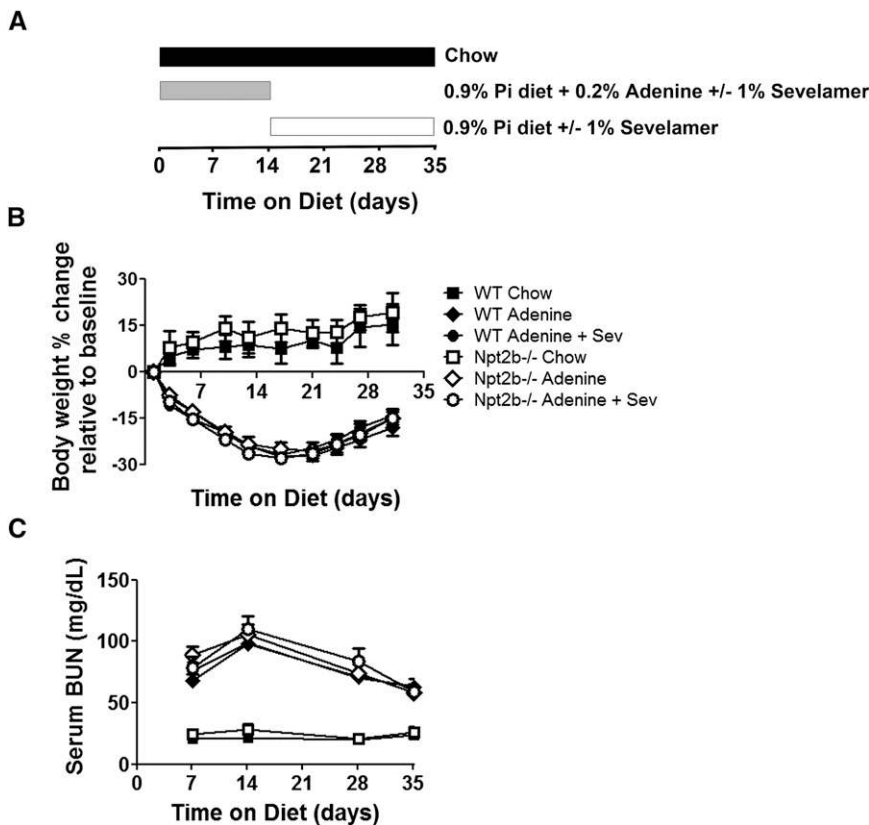


Figure 2. Phenotypic characteristics of uremic mouse model. (A) Study design illustrating the different diets and adenine withdrawal 2 weeks after uremic induction. This design is applicable to all studies presented in this article. (B) Animal weights were measured throughout the study. Differences were not observed between normal WT mice (closed symbols) and Npt2b^{-/-} mice (open symbols). All uremic groups lost significant weight ($P < 0.05$) to the same extent without observable effects of sevelamer carbonate (Sev) treatment. (C) Kidney function was assessed by serum BUN levels. Serum BUN was significantly elevated between normal and uremic mice ($P < 0.05$). BUN levels peaked at 2 weeks during adenine treatment, which then decreased after adenine withdrawal. Differences in serum creatinine were not observed between genotypes or binder treatments. Data expressed as mean \pm SEM. $n = 8-15$ /group.

Phosphate Lowering Improved Bone Health

Adenine-treated WT and Npt2b^{-/-} mice exhibited high turnover bone disease with significant elevations in bone formation and mineral apposition rates (Figure 6, A and B). A significant reduction in the mineral apposition rate led to a consistent trend toward reduced bone formation in binder-treated relative to untreated uremic Npt2b^{-/-} mice (Figure 6, A and B). In contrast, binder treatment did not affect bone formation and mineral apposition rate in uremic WT mice (Figure 6, A and B). Elevations in osteoid surface area were also noted in all adenine-treated groups but this parameter was not altered by Npt2b deletion and/or sevelamer treatment (Figure 6C). Although significant differences in osteoclast number were not observed in the adenine-treated mice relative to their chow controls, there was a statistically significant decrease in osteoclast

numbers in uremic Npt2b^{-/-} compared with WT mice (Figure 6D). Sevelamer treatment led to a significant decrease in osteoclast number in uremic WT mice with a trend toward further decrease in Npt2b^{-/-} mice ($P = 0.06$) (Figure 6D).

DISCUSSION

Recently, we and others have demonstrated an important role of Npt2b in maintaining normal phosphate homeostasis.^{6,15} Multiple studies provide indirect evidence that Npt2b may also participate in CKD-associated hyperphosphatemia.^{6,11,13,16-18} To directly assess the therapeutic potential of targeting Npt2b, we evaluated the long-term effect of Npt2b deletion in a chronic CKD model. Using a modified adenine model in which progression of renal failure was limited by adenine withdrawal while allowing development of hyperphosphatemia and high turnover bone disease, we confirmed sustained decrease in serum phosphate levels in the Npt2b^{-/-} mice.

Our data extend recent findings using an acute uremic model demonstrating that a 50% reduction in Npt2b expression could prevent rapid development of hyperphosphatemia.¹⁵ Unlike the study reported by Ohi *et al.*, normalization of serum phosphorus in our model was observed only with concurrent binder treatment.¹⁵ In chronic disease, renal osteodystrophy is a known contributor to serum phosphate with the link between poor bone health and cardiovascular events well documented.¹⁹⁻²¹ Therefore, in our 5-week model, high bone turnover may contribute to the phosphate burden requiring more robust phosphate management. The differences in the magnitude of phosphate control may also be related to the higher bioavailable dietary phosphate in our study, leading to a greater contribution of passive transport and increased phosphate load. This point is exemplified by our data showing that although serum phosphate was reduced in uremic Npt2b^{-/-}, changes in urinary and fecal excretion were not observed. The high dietary phosphate levels could have also prevented the compensatory increases in Npt2a protein expression and urinary phosphate excretion that we previously reported (Figure 3D).⁶

Despite these experimental caveats, correlation analysis of serum BUN with serum phosphate of WT and Npt2b^{-/-} mice demonstrated that Npt2b deletion shifts the phosphate slope to the right (Figure 4A). This analysis highlights the effects of

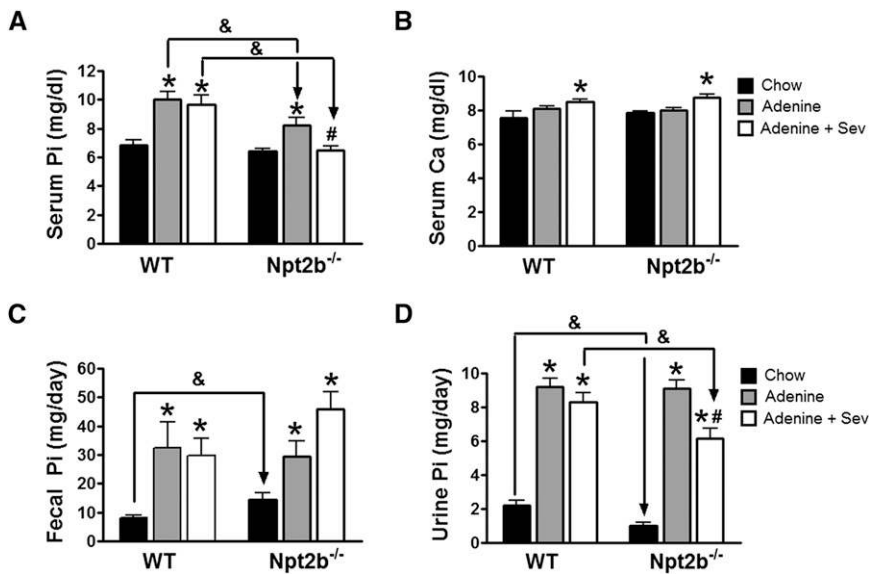


Figure 3. Phosphate balance restored in *Npt2b*^{-/-} mice. Serum, urine, and fecal phosphate and serum calcium were measured at end of life. (A) Serum phosphate (Pi) was significantly elevated in uremic WT and this effect was attenuated in uremic *Npt2b*^{-/-} mice. Sevelamer carbonate (Sev) treatment normalized serum phosphate in uremic *Npt2b*^{-/-} mice, whereas no statistically significant differences were observed in WT mice. (B) Serum calcium (Ca) was not different between WT and *Npt2b*^{-/-} mice, although a slight elevation in serum calcium was observed with sevelamer carbonate treatment. (C) Fecal phosphate excretion is elevated in normal *Npt2b*^{-/-} mice. Uremic mice on a high-phosphate diet led to a significant increase in phosphate output. Sevelamer carbonate treatment further increased phosphate excretion in uremic *Npt2b*^{-/-} mice. (D) Urine phosphate is reduced in normal *Npt2b*^{-/-} mice relative to WT mice. Uremic mice on a high-phosphate diet had a significant increase in urinary phosphate excretion. Sevelamer carbonate treatment significantly decreased urinary output in uremic *Npt2b*^{-/-} mice relative to untreated *Npt2b*^{-/-} mice and treated WT mice. Data expressed as mean \pm SEM. * $P < 0.05$ versus chow; # $P < 0.05$ versus adenine; & $P < 0.05$ versus WT. $n = 8$ – 15 /group.

decreased phosphate absorption on serum levels despite the similar degree of renal dysfunction between WT and *Npt2b*^{-/-} mice (Figure 4A). Analysis of the slope of best-fit linear regression for the different treatment groups demonstrated the additive effect of *Npt2b* deletion with sevelamer carbonate in controlling serum phosphate (Figure 4B).

The use of the adenine-induced uremia model has been challenged by previous rat studies demonstrating histopathological changes in the intestine.²² In our modified adenine mouse model, intestinal tissue appeared normal by histologic analysis (Figure 1B). Furthermore, we have validated our finding that *Npt2b* attenuates hyperphosphatemia in renal ablated mice, a second uremic model (Supplemental Figure 2).

An important question is whether sufficient *Npt2b* protein exists in the presence of renal failure to warrant targeting it therapeutically. Our studies utilizing immunofluorescence demonstrate that significant *Npt2b* expression was present in the intestinal brush border in all uremic WT groups despite animal to animal expression variability (Figure 1, A and C).

These results are somewhat consistent with studies in 5/6 nephrectomized rats in which *Npt2b* expression and phosphate uptake were unaltered in the uremic state.¹⁶

Recent data in a progressive genetic CKD rat model showed that animals treated with 3% sevelamer carbonate or calcium carbonate had a decrease in intestinal phosphate flux.¹⁷ A potentially important observation in our study was that considerable interanimal variability was observed within each animal group as detected by immunoblot analysis (Figure 1C) or immunofluorescence. However, quantitation of protein expression by immunoblot demonstrated that 1% sevelamer treatment in uremic WT mice led to a significant increase in *Npt2b* protein expression (Figure 1D). These results might also explain why binder treatment was less efficient in phosphate control in uremic WT mice compared with uremic *Npt2b*^{-/-}. This variability in expression may be partially explained by experimental design, in which the timing of last feeding relative to tissue collection between mice may have been different due to the lack of fasting before sacrifice. This is in line with recent studies demonstrating post-transcriptional changes in *Npt2b* after acute alterations in dietary phosphate intake.¹⁸

It is well known that the key hormones regulating calcium and phosphate homeostasis become dysregulated in CKD. As expected, serum PTH levels were equivalently elevated in uremic WT and *Npt2b*^{-/-} mice (Figure 5A). Sevelamer carbonate treatment did not alter serum PTH in WT mice and was associated with modestly decreased levels in uremic *Npt2b*^{-/-} mice. As previously reported, FGF23 levels were attenuated in *Npt2b*^{-/-} compared with WT mice (Figure 5B).⁶ Differential FGF23 levels between WT and *Npt2b*^{-/-} uremic mice remained although statistical significance was not achieved. Binder treatment was associated with a trend toward reduced FGF23 in WT mice, whereas a significant decrease was observed in *Npt2b*^{-/-} mice. The pattern of changes in FGF23 levels in the *Npt2b*^{-/-} mice mirrored relative changes in phosphate absorption as they corresponded to parallel changes in fecal, serum, and urinary phosphate parameters. Thus, in our study, the greatest control of phosphate was associated with the most significant FGF23 changes. These observations suggest that reduction of hyperphosphatemia is a more robust modulator of FGF23 than PTH.^{23–27} It has been recently demonstrated that elevated FGF23 directly contributes to the pathogenesis of left ventricular hypertrophy.²³

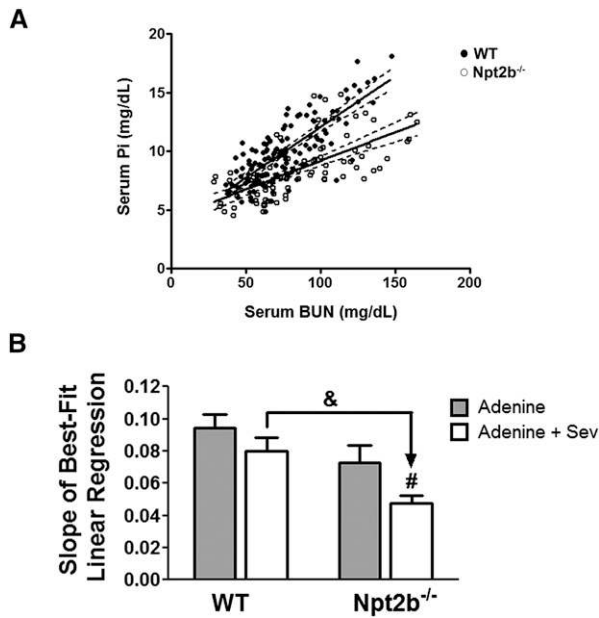


Figure 4. Correlation analysis between serum BUN and serum phosphate. (A) Linear regression analysis between all WT mice (closed symbols) and Npt2b^{-/-} mice (open symbols) reveals a significant difference in the correlation between serum phosphate (Pi) and serum BUN; WT ($R^2=0.62$) and Npt2b^{-/-} mice ($R^2=0.45$) ($P<0.05$). (B) Slope of best-fit linear regression analysis for the uremic groups demonstrates additive effects of Npt2b deletion and sevelamer carbonate (Sev) treatment on serum phosphate regulation. Data expressed as mean \pm SEM. # $P<0.05$ versus adenine; & $P<0.05$ versus WT. $n=8-15$ /group.

Bone disease is a characteristic feature of CKD-mineral bone disorder.²⁸⁻³⁰ Evidence derived from classic clinical radiolabel studies suggests that the inability of bone to serve as a buffer for excess calcium and phosphate contributes to serum phosphate elevations and may lead to deposition of excess mineral in soft tissues.^{31,32} We therefore determined the effect of Npt2b deletion on bone disease in the adenine mouse model. Classic features of high turnover, including increased bone formation rates, elevated mineral apposition rates, and increased osteoid surface, were observed in uremic mice as an apparent consequence of elevated PTH (Figure 6). Importantly, sevelamer treatment was associated with a reduction in both osteoclast activity and number, suggesting that modulation of systemic phosphate is linked to osteoclast function. These effects were more significant in binder-treated uremic Npt2b^{-/-}, the condition providing greatest phosphate control (Figure 6D). Our results are consistent with published findings demonstrating that in addition to its contribution toward redistribution of systemic phosphate levels, bone itself is also responsive to phosphate levels. Several clinical studies examining binder-treated ESRD patients have shown benefits of phosphate management on bone.^{33,34} In the ovariectomized rat model of high turnover with normal kidney function, sevelamer treatment was associated with reduced osteoclast

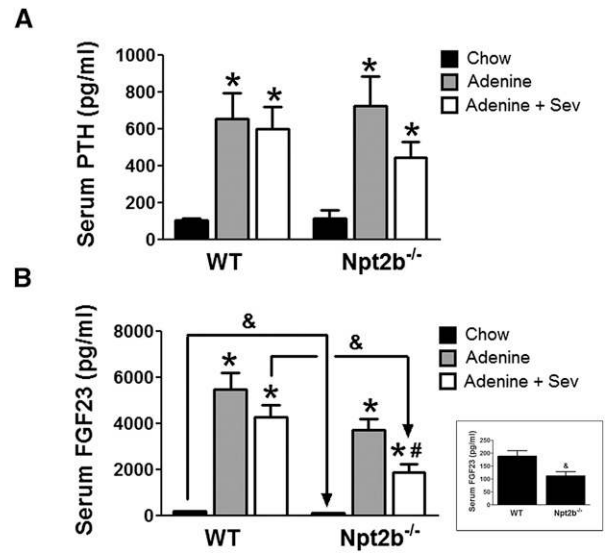


Figure 5. FGF23 but not PTH was altered in uremic Npt2b^{-/-} mice. (A) Serum PTH is unchanged in normal Npt2b^{-/-} relative to WT mice. Uremic mice on a high-phosphate diet led to a significant increase in serum PTH with no differences observed between WT and Npt2b^{-/-} mice. Sevelamer carbonate (Sev) treatment did not significantly alter serum PTH levels. (B) Serum FGF23 levels are decreased in normal Npt2b^{-/-} relative to WT mice (inset). Uremic mice on a high-phosphate diet had significantly higher serum FGF23 relative to nonuremic mice. A trend of reduced levels was observed in the presence of Npt2b deletion or with sevelamer treatment of WT mice. Statistical significance was reached in sevelamer-treated Npt2b^{-/-} mice. Data expressed as mean \pm SEM. * $P<0.05$ versus chow; # $P<0.05$ versus adenine; & $P<0.05$ versus WT. $n=8-15$ /group.

number and activity leading to improved bone quality.³⁵ In other studies, when mice were placed on a low-phosphate diet, decreased osteoclast numbers were observed, whereas a high-phosphate diet was associated with enhanced bone resorption.^{36,37} Zhang *et al.* demonstrated that in *Dmp1* hypophosphatemic knockout mice, a reduction in the number of osteoclasts was observed.³⁸ Importantly, normalization of serum phosphate by FGF23 antibody administration resulted in increased osteoclast numbers.³⁸ These changes appeared to be independent of alterations in PTH or 1,25 vitamin D₃ but were associated with corresponding changes in the ratio of receptor activator of NF κ B ligand to osteoprotegerin. Recently, we provided evidence in a progressive genetic model of CKD that repression of the β -catenin signaling in osteocytes was associated with an increase in the ratio of receptor activator of NF κ B ligand to osteoprotegerin.³⁹ Because these changes were independent of observable changes in serum phosphate or PTH, it remains to be determined whether phosphate contributes directly or indirectly to osteocyte regulation of osteoclast activity in the context of CKD.

Several lines of evidence suggest that the benefits of phosphate lowering on cardiovascular health include reduction

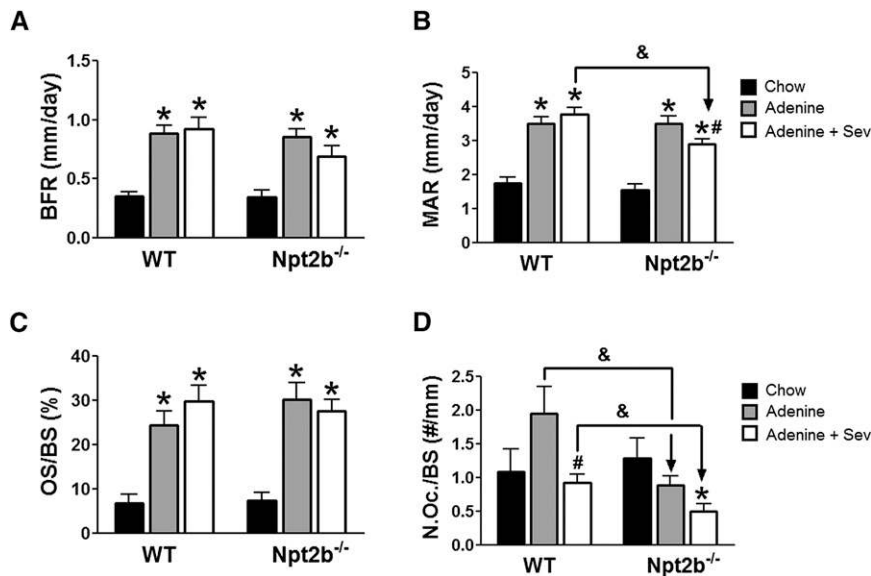


Figure 6. Bone parameters altered in uremic *Npt2b*^{-/-} mice. (A) Bone formation rates (BFR) were elevated in uremic WT and *Npt2b*^{-/-} mice. Sevelamer carbonate (Sev) was associated with a trend for reduced BFR in uremic *Npt2b*^{-/-} mice. (B) Mineral apposition rates (MAR) were significantly elevated in uremic WT and *Npt2b*^{-/-} mice. Sevelamer carbonate significantly reduced MAR in uremic *Npt2b*^{-/-} mice. (C) Osteoid surface over bone surface (OS/BS) was elevated in uremic WT and *Npt2b*^{-/-} mice. Sevelamer carbonate did not alter OS/BS in uremic WT and *Npt2b*^{-/-} mice. (D) Number of osteoclasts over bone surface (N.Oc./BS) was slightly elevated in uremic WT mice relative to normal mice. No increase was observed in uremic *Npt2b*^{-/-} mice. Sevelamer carbonate treatment reduced the number of osteoclasts in uremic WT and *Npt2b*^{-/-} mice. Data expressed as mean \pm SEM. **P*<0.05 versus chow; #*P*<0.05 versus adenine; &*P*<0.05 versus WT. *n*=7–9/group.

of vascular stiffness and calcification.^{40,41} We did not observe vascular calcification in our adenine-treated mice, because the C57BL/6 mouse strain used in this study is known to be resistant to the development of overt vascular calcification.⁴²

Our data also raise the possibility that reducing bone turnover may in turn contribute to the decreased serum phosphate in uremic *Npt2b*^{-/-} mice without altering phosphate excretion. The attenuation of high turnover may lead to redistribution or maintenance of phosphate and calcium in the bone, thereby decreasing the systemic phosphate burden. Our results suggest that along with inhibition of phosphate absorption in the gut, restoration of bone buffering capacity may be important to achieving phosphate control in the setting of CKD. Taken together, our studies demonstrate that modulating phosphate through the intestinal sodium-dependent phosphate cotransporter, *Npt2b* attenuated the hyperphosphatemia observed in control animals and that sevelamer carbonate treatment had an additional benefit in maintaining serum phosphate in the normal range. These effects were associated with reduced serum FGF23 and improvement in bone health. Finally, our studies support *Npt2b* as a molecular target for the development of novel therapeutic strategies for hyperphosphatemia. *Npt2b*

inhibition in addition to dietary phosphorus binders may represent a new paradigm for improved phosphorus management in CKD.

CONCISE METHODS

Mice

All studies were approved by the institutional animal care committee. Mice were maintained in a virus- and parasite-free barrier facility and exposed to a 12-hour light/dark cycle. The generation of the conditional knockout mice has been previously described.⁶ Experiments were initiated 1 week after induction of *Npt2b* knockdown with tamoxifen as previously described.⁶ Unless otherwise specified, animals were maintained on standard rodent chow diet (PicoLab Rodent Diet 20, #5053; LabDiet, St. Louis, MO) containing 0.63% phosphate, 0.81% calcium with 2.2 IU/g vitamin D₃. To induce uremia, 0.2% adenine was added to a casein-based synthetic diet containing 0.9% phosphate and 0.6% calcium (#110457; Dyets Inc., Bethlehem, PA) for 2 weeks (Figure 2A). Then adenine was withdrawn but the mice were kept on the casein diet for another 3 weeks. Binder-treated groups received 1% sevelamer carbonate (Genzyme, Cambridge, MA) mixed in diet (Figure 2A). Animal numbers per group used are indicated in the figure legends.

Surgical Renal Ablation

CKD was induced in WT and *Npt2b*^{-/-} mice by the procedure previously described by Gagnon and Duguid.⁴³ Briefly, electrocautery of the entire surface of the right kidney except for a 2 mm of intact tissue around the hilum was followed by left nephrectomy 2 weeks afterward. The casein-based high-phosphate diet was initiated after the second surgery. In the sham-operated animals, the kidneys were temporarily exposed but were not manipulated.

Histology

Kidney and ileum (last 10 mm) were harvested and fixed for 24 hours in 10% formalin, placed in 70% ethanol, embedded in paraffin, and sectioned. Sections were dewaxed in xylene, rehydrated by ethanol gradient, and stained in hematoxylin and eosin or von Kossa. For bone analysis mice were given an intraperitoneal injection of calcein (15 mg/kg) 8 days before sacrifice and alizarin red (40 mg/kg) 3 days before sacrifice. Femurs were fixed in 40% alcohol and processed in methyl methacrylate. Each femur was sectioned at two levels per block separated by 100 μ m in the ventral/dorsal plane. At each level, five serial 5- μ m sections were obtained. Goldner's Trichrome and von Kossa sections were analyzed for static measurements using the Osteo II Bioquant system (Bioquant, Nashville, TN). Unstained serial sections were used for dynamic measurements using the Osteo II Bioquant system. Nomenclature is in agreement with recommendations by Parfitt *et al.*⁴⁴

Immunofluorescence

Paraffin slides were dewaxed and rehydrated followed by antigen retrieval using sodium citrate solution (pH 9.9; Dako, Carpinteria, CA) and placed in pressure cooker for 15 minutes. Cooled slides were blocked in 5% goat serum/0.1% Triton 100/PBS for 1 hour. Ileum sections were incubated with rabbit anti-mouse Npt2b (1 μ g/ml), raised against a carboxy-terminal peptide (CQVEVLSMKALSNTTVF). Blocking and primary antibody incubations were in 5% goat serum/PBS base. Goat anti-rabbit IgG conjugated to Alexa Fluor 488 (Invitrogen, Grand Island, NY) was used to detect rabbit anti-mouse primary and phalloidin conjugated to Alexa Fluor 594 (Invitrogen) was used to detect actin filaments. Coverslips were mounted with VectaShield hard set mounting media (VectorLabs, Burlingame, CA). Images were captured on a Zeiss AxioVert 200 microscope.

Immunoblot Analyses

Tissue isolated as described above was homogenized in tissue protein extraction reagent (T-PER) (Thermo Fisher Scientific, Rockford, IL) in the presence of complete protease inhibitors (Roche Diagnostics, Indianapolis, IN) and phenylmethylsulfonyl fluoride (Sigma, St. Louis, MO). Total lysate from ileum (40 μ g) were subjected to electrophoresis on Nu-PAGE gel (Invitrogen) and detected using rabbit anti-mouse Npt2b (1 μ g/ml). Anti-rabbit IgG, horseradish peroxidase-linked antibody (Cell Signal Technologies) was used as a secondary antibody. Enhanced chemiluminescence (Pierce Supersignal West Dura) was used as detection method. Blots were normalized to β -actin primary antibody directly conjugated to horseradish peroxidase (Cell Signal Technologies). Autoradiographs were scanned, and the ratio of Npt2b to β -actin was quantified by image analysis, using ImageJ software (National Institutes of Health, Bethesda, MD).

Serum and Urine Analyses

Whole blood was collected under isoflurane anesthesia *via* retro-orbital bleed, incubated for 20 minutes at room temperature, and then centrifuged at 4°C. Serum was aliquoted and frozen at -80°C for subsequent analysis. Animals were placed in metabolic cages in which urine and feces were collected over a 24-hour period. Urine was centrifuged to remove particulates and the resultant supernatant volume recorded. All serum and urine phosphate, calcium, BUN, and creatinine (enzymatic method) were measured on an Integra 400 bioanalyzer (Roche Diagnostics, Indianapolis, IN). Intact PTH (Immutopics, San Clemente, CA) and intact FGF23 (Kainos, Tokyo, Japan) ELISAs were performed according to the manufacturers' instructions.

Fecal Phosphate Analyses

Stool samples were collected over a 24-hour period and contaminating food was removed. Fecal samples were weighed and lyophilized overnight. The dry weight of stool sample was reconstituted in 0.6 M hydrochloric acid (Sigma) to a final concentration of 50 mg/ml for 3 days under gentle rotation. On the second day of extraction, samples were homogenized, mixed for 24 hours, and then centrifuged at 2000 RCF for 5 minutes to remove particulate matter. A portion of supernatant was diluted 1:100 with HPLC (Baker) grade water.

Fecal phosphate was quantified according to the manufacturer's protocol (Stanbio Laboratories).

Statistical and Correlation Analyses

All serum, urine, and fecal biochemistry data were calculated using the Man-Whitney nonparametric test. The *t* test was used to analyze significance between two groups for all other endpoints. *P* values <0.05 was considered significant.

Correlation analysis between serum phosphate and BUN was performed using linear regression for each genotype (combining chow, adenine, and adenine and sevelamer treatment) and plotted on the same graph. Subgroup analysis for each of the treatment groups was performed by performing a linear regression for each of the uremic groups and the slope of best-fit plotted.

ACKNOWLEDGMENTS

We thank the following colleagues from Genzyme: William Weber for imaging analysis, Leah Curtin for colony management, and Michael Phipps and Matthew DeRiso for genotyping.

A portion of this work was presented at the 2011 Annual Meeting of the American Society of Nephrology, November 10–13, 2011, in Philadelphia, Pennsylvania.

DISCLOSURES

All authors are employees of Genzyme, a Sanofi company.

REFERENCES

- Dhingra R, Sullivan LM, Fox CS, Wang TJ, D'Agostino RB Sr, Gaziano JM, Vasan RS: Relations of serum phosphorus and calcium levels to the incidence of cardiovascular disease in the community. *Arch Intern Med* 167: 879–885, 2007
- Block GA, Hulbert-Shearon TE, Levin NW, Port FK: Association of serum phosphorus and calcium x phosphate product with mortality risk in chronic hemodialysis patients: A national study. *Am J Kidney Dis* 31: 607–617, 1998
- Cramer CF: Progress and rate of absorption of radiophosphorus through the intestinal tract of rats. *Can J Biochem Physiol* 39: 499–503, 1961
- Kayne LH, D'Argenio DZ, Meyer JH, Hu MS, Jamgotchian N, Lee DB: Analysis of segmental phosphate absorption in intact rats. A compartmental analysis approach. *J Clin Invest* 91: 915–922, 1993
- McHardy GJR, Parsons DS: The absorption of inorganic phosphate from the small intestine of the rat. *Q J Exp Physiol* 41: 398–409, 1956
- Sabbagh Y, O'Brien SP, Song W, Boulanger JH, Stockmann A, Arbeeney C, Schiavi SC: Intestinal npt2b plays a major role in phosphate absorption and homeostasis. *J Am Soc Nephrol* 20: 2348–2358, 2009
- Sampathkumar K, Sooraj YS, Ajeshkumar RP: Extended release nicotinic acid is a promising agent for phosphate control in hemodialysis. *Kidney Int* 69: 1281, 2006
- Musso CG, Reynaldi MJ, Aparicio C, Frydenlund S, Imperiali N, Algranati L: Hyperphosphatemia and nicotinic acid in peritoneal dialysis patients. *Int Urol Nephrol* 40: 229–230, author reply 231, 2008

9. Takahashi Y, Tanaka A, Nakamura T, Fukuwatari T, Shibata K, Shimada N, Ebihara I, Koide H: Nicotinamide suppresses hyperphosphatemia in hemodialysis patients. *Kidney Int* 65: 1099–1104, 2004
10. Cheng SC, Young DO, Huang Y, Delmez JA, Coyne DW: A randomized, double-blind, placebo-controlled trial of niacinamide for reduction of phosphorus in hemodialysis patients. *Clin J Am Soc Nephrol* 3: 1131–1138, 2008
11. Katai K, Tanaka H, Tatsumi S, Fukunaga Y, Genjida K, Morita K, Kuboyama N, Suzuki T, Akiba T, Miyamoto K, Takeda E: Nicotinamide inhibits sodium-dependent phosphate cotransport activity in rat small intestine. *Nephrol Dial Transplant* 14: 1195–1201, 1999
12. Eto N, Miyata Y, Ohno H, Yamashita T: Nicotinamide prevents the development of hyperphosphatemia by suppressing intestinal sodium-dependent phosphate transporter in rats with adenine-induced renal failure. *Nephrol Dial Transplant* 20: 1378–1384, 2005
13. Caldas YA, Giral H, Cortázar MA, Sutherland E, Okamura K, Blaine J, Sorribas V, Koepsell H, Levi M: Liver X receptor-activating ligands modulate renal and intestinal sodium-phosphate transporters. *Kidney Int* 80: 535–544, 2011
14. Cho KH, Kim HJ, Rodriguez-Iturbe B, Vaziri ND: Niacin ameliorates oxidative stress, inflammation, proteinuria, and hypertension in rats with chronic renal failure. *Am J Physiol Renal Physiol* 297: F106–F113, 2009
15. Ohi A, Hanabusa E, Ueda O, Segawa H, Horiba N, Kaneko I, Kuwahara S, Mukai T, Sasaki S, Tominaga R, Furutani J, Aranami F, Ohtomo S, Oikawa Y, Kawase Y, Wada NA, Tachibe T, Kakefuda M, Tateishi H, Matsumoto K, Tatsumi S, Kido S, Fukushima N, Jishage KI, Miyamoto KI: Inorganic phosphate homeostasis in sodium-dependent phosphate co-transporter Npt2b+/- mice. *Am J Physiol Renal Physiol* 301: F1105–F1113, 2011
16. Marks J, Churchill LJ, Srai SK, Biber J, Murer H, Jaeger P, Debnam ES, Unwin RJ; Epithelial Transport and Cell Biology Group: Intestinal phosphate absorption in a model of chronic renal failure. *Kidney Int* 72: 166–173, 2007
17. Moe SM, Radcliffe JS, White KE, Gattone VH 2nd, Seifert MF, Chen X, Aldridge B, Chen NX: The pathophysiology of early-stage chronic kidney disease-mineral bone disorder (CKD-MBD) and response to phosphate binders in the rat. *J Bone Miner Res* 26: 2672–2681, 2011
18. Giral H, Caldas Y, Sutherland E, Wilson P, Breusegem S, Barry N, Blaine J, Jiang T, Wang XX, Levi M: Regulation of rat intestinal Na-dependent phosphate transporters by dietary phosphate. *Am J Physiol Renal Physiol* 297: F1466–F1475, 2009
19. Hruska KA, Mathew S, Lund RJ, Memon I, Saab G: The pathogenesis of vascular calcification in the chronic kidney disease mineral bone disorder: The links between bone and the vasculature. *Semin Nephrol* 29: 156–165, 2009
20. Malluche HH, Mawad H, Monier-Faugere MC: The importance of bone health in end-stage renal disease: Out of the frying pan, into the fire? *Nephrol Dial Transplant* 19[Suppl 1]: i9–i13, 2004
21. Moe S, Drüeke T, Cunningham J, Goodman W, Martin K, Olgaard K, Ott S, Sprague S, Lameire N, Eknoyan G; Kidney Disease: Improving Global Outcomes (KDIGO): Definition, evaluation, and classification of renal osteodystrophy: A position statement from Kidney Disease: Improving Global Outcomes (KDIGO). *Kidney Int* 69: 1945–1953, 2006
22. Lacour B, Lucas A, Auchère D, Ruellan N, de Serre Patey NM, Drüeke TB: Chronic renal failure is associated with increased tissue deposition of lanthanum after 28-day oral administration. *Kidney Int* 67: 1062–1069, 2005
23. Faul C, Amaral AP, Oskouei B, Hu MC, Sloan A, Isakova T, Gutiérrez OM, Aguillon-Prada R, Lincoln J, Hare JM, Mundel P, Morales A, Scialla J, Fischer M, Soliman EZ, Chen J, Go AS, Rosas SE, Nessel L, Townsend RR, Feldman HI, St John Sutton M, Ojo A, Gadegbeku C, Di Marco GS, Reuter S, Kentrup D, Tiemann K, Brand M, Hill JA, Moe OW, Kuro-O M, Kusek JW, Keane MG, Wolf M: FGF23 induces left ventricular hypertrophy. *J Clin Invest* 121: 4393–4408, 2011
24. Kendrick J, Cheung AK, Kaufman JS, Greene T, Roberts WL, Smits G, Chonchol M; HOST Investigators: FGF-23 associates with death, cardiovascular events, and initiation of chronic dialysis. *J Am Soc Nephrol* 22: 1913–1922, 2011
25. Mirza MA, Larsson A, Lind L, Larsson TE: Circulating fibroblast growth factor-23 is associated with vascular dysfunction in the community. *Atherosclerosis* 205: 385–390, 2009
26. Mirza MA, Larsson A, Melhus H, Lind L, Larsson TE: Serum intact FGF23 associate with left ventricular mass, hypertrophy and geometry in an elderly population. *Atherosclerosis* 207: 546–551, 2009
27. Wolf M, Molnar MZ, Amaral AP, Czira ME, Rudas A, Ujaszasi A, Kiss I, Rosivall L, Kosa J, Lakatos P, Kovesdy CP, Mucsi I: Elevated fibroblast growth factor 23 is a risk factor for kidney transplant loss and mortality. *J Am Soc Nephrol* 22: 956–966, 2011
28. Parfitt AM: Renal bone disease: A new conceptual framework for the interpretation of bone histomorphometry. *Curr Opin Nephrol Hypertens* 12: 387–403, 2003
29. Kidney Disease: Improving Global Outcomes (KDIGO) CKD-MBD Work Group: KDIGO clinical practice guideline for the diagnosis, evaluation, prevention, and treatment of chronic kidney disease-mineral and bone disorder (CKD-MBD). *Kidney Int Suppl* 113: S1–S130, 2009
30. Felsenfeld A, Torres A: Bone histomorphometry in renal osteodystrophy. In: *The Spectrum of Mineral and Bone Disorders in Chronic Kidney Disease*, 2nd Ed., edited by Olgaard K, Silver J, Isidro B. Salusky IB, New York, Oxford University Press, 2010, 145–172
31. Kurz P, Monier-Faugere MC, Bogner B, Werner E, Roth P, Vlachojannis J, Malluche HH: Evidence for abnormal calcium homeostasis in patients with adynamic bone disease. *Kidney Int* 46: 855–861, 1994
32. Parfitt AM: Misconceptions (3): Calcium leaves bone only by resorption and enters only by formation. *Bone* 33: 259–263, 2003
33. Barreto DV, Barreto FC, de Carvalho AB, Cuppari L, Draibe SA, Dalboni MA, Moyses RM, Neves KR, Jorgetti V, Miname M, Santos RD, Canziani ME: Phosphate binder impact on bone remodeling and coronary calcification—results from the BRiC study. *Nephron Clin Pract* 110: c273–c283, 2008
34. Ferreira A, Frazão JM, Monier-Faugere MC, Gil C, Galvao J, Oliveira C, Baldaia J, Rodrigues I, Santos C, Ribeiro S, Hoenger RM, Duggal A, Malluche HH; Sevelamer Study Group: Effects of sevelamer hydrochloride and calcium carbonate on renal osteodystrophy in hemodialysis patients. *J Am Soc Nephrol* 19: 405–412, 2008
35. Sampath TK, Simic P, Moreno S, Bukanov N, Draca N, Kufner V, Tikvica A, Blair A, Semenski D, Brncic M, Burke SK, Vukicevic S: Sevelamer restores bone volume and improves bone microarchitecture and strength in aged ovariectomized rats. *Endocrinology* 149: 6092–6102, 2008
36. Koyama Y, Rittling SR, Tsuji K, Hino K, Salincamboriboon R, Yano T, Taketani Y, Nifuji A, Denhardt DT, Noda M: Osteopontin deficiency suppresses high phosphate load-induced bone loss via specific modulation of osteoclasts. *Endocrinology* 147: 3040–3049, 2006
37. Hayashibara T, Hiraga T, Sugita A, Wang L, Hata K, Ooshima T, Yoneda T: Regulation of osteoclast differentiation and function by phosphate: Potential role of osteoclasts in the skeletal abnormalities in hypophosphatemic conditions. *J Bone Miner Res* 22: 1743–1751, 2007
38. Zhang R, Lu Y, Ye L, Yuan B, Yu S, Qin C, Xie Y, Gao T, Drezner MK, Bonewald LF, Feng JQ: Unique roles of phosphorus in endochondral bone formation and osteocyte maturation. *J Bone Miner Res* 26: 1047–1056, 2011
39. Sabbagh Y, Gracioli FG, O'Brien S, Tang W, Dos Reis LM, Ryan S, Phillips L, Boulanger J, Song W, Bracken C, Liu S, Ledbetter S, Dechow P, Canziani ME, Carvalho AB, Jorgetti V, Moyses RM, Schiavi SC: Repression of osteocyte Wnt/beta-catenin signaling is an early event in the progression of renal osteodystrophy. *J Bone Miner Res* 27: 1757–1772, 2012
40. Goodman WG, Goldin J, Kuizon BD, Yoon C, Gales B, Sider D, Wang Y, Chung J, Emerick A, Greaser L, Elashoff RM, Salusky IB: Coronary-artery calcification in young adults with end-stage renal disease who are undergoing dialysis. *N Engl J Med* 342: 1478–1483, 2000

41. Raggi P, Boulay A, Chasan-Taber S, Amin N, Dillon M, Burke SK, Chertow GM: Cardiac calcification in adult hemodialysis patients. A link between end-stage renal disease and cardiovascular disease? *J Am Coll Cardiol* 39: 695–701, 2002
42. Westenfeld R, Schäfer C, Smeets R, Brandenburg VM, Floege J, Ketteler M, Jahnke-Dechent W: Fetuin-A (AHSG) prevents extraosseous calcification induced by uraemia and phosphate challenge in mice. *Nephrol Dial Transplant* 22: 1537–1546, 2007
43. Gagnon RF, Duguid WP: A reproducible model for chronic renal failure in the mouse. *Urol Res* 11: 11–14, 1983
44. Parfitt AM, Drezner MK, Glorieux FH, Kanis JA, Malluche H, Meunier PJ, Ott SM, Recker RR; Report of the ASBMR Histomorphometry Nomenclature Committee: Bone histomorphometry: Standardization of nomenclature, symbols, and units. *J Bone Miner Res* 2: 595–610, 1987

This article contains supplemental material online at <http://jasn.asnjournals.org/lookup/suppl/doi:10.1681/ASN.2011121213/-/DCSupplemental>.